Analytic Expressions for the Reflection Delay, Penetration Depth, and Absorptance of Quarter-Wave Dielectric Mirrors

Dubravko I. Babic and Scott W. Corzine

Abstract—**In this paper we analyze the operation of high-reflectivity quarter-wave (QW) dielectric mirrors at the band-stop center (Bragg) frequency, relevant for the design of small-cavity optoelectronic structures. We discuss the mirror penetration depth from the standpoints of reflection delay and energy storage in the quarter-wave mirrors and derive *exact* analytic expressions for the penetration depth at the mirror center frequency based on both definitions. We show that, in general, the two models yield different expressions for the penetration depth, but for certain practical cases the difference is negligible. We also present the mathematical analysis and expressions for the absorptance and the peak reflectivity of a dielectric mirror with weak material absorption. The quarter-wave mirrors have typically been analyzed using coupled-wave theory, which applies to mirrors with small index differences, or by exact numerical calculation using the transmission matrix approach. In this paper we derive expressions for the penetration depth and mirror reflection delay that are valid for *arbitrary* material refractive index combinations and *any* number of layers, and are therefore applicable both for semiconductor and amorphous dielectric mirrors. The use of our results is illustrated for a typical vertical cavity surface-emitting laser structure.**

I. Introduction

THE realization of high-reflectivity laser mirrors typically involves the use of one or more dielectric quarter-wave stacks to achieve a desired reflectivity and bandwidth [1], [2]. Due to the distributed nature of a quarter-wave (QW) stack, these mirrors exhibit phase dispersion and a finite delay upon reflection. The dispersion is responsible for pulse broadening and distortion [2], whereas the reflection delay adds to the laser cavity round-trip time. The storage of electromagnetic energy in a distributed reflector is also a factor of interest in the case of small-cavity structures where the cavity volume and the cavity round-trip time are of comparable magnitude as the mirror storage and the reflection delay. The primary examples here are vertical cavity surface-emitting lasers (VCSEL) [3] and vertical Fabry–Perot modulators [4]. It has been common practice [5] to account for both the reflection delay time and the energy storage in distributed laser mirrors by defining a quantity called *penetration depth* as the depth inside the mirror at which the optical pulse *appears* to reflect, or the energy falls of to $1/e$ of its initial value. The sum of the physical cavity length and the mirror penetration depth gives the *effective* cavity length. The *penetration depth* has typically been calculated using coupled-wave theory (CWT) [6], [7], which applies in the cases when the difference in the mirror material refractive indexes is small. Except for the exact numerical calculation using the transmission matrix approach [8], [9] there has not been any simple way of predicting the reflection delay and the energy penetration for mirrors involving materials with arbitrarily large refractive index differences. Furthermore, it has not been clearly stated that the two definitions of the penetration depth: the definition by reflection delay and by energy storage, in fact lead to two different penetration depths.

In this paper we discuss these definitions and derive *exact* analytic expressions for both the reflection delay and the energy penetration depth of a quarter-wave mirror (QWM) at the mirror center frequency that is valid for arbitrary large refractive index differences and number of layers. We will also use the energy penetration depth concept to determine a first-order linear approximation for the reduction of the mirror peak reflectivity of the QWM as a function of the mirror material parameters and the number of layers. The obtained expression can be applied in the limit of small loss.

II. Background

The term *quarter-wave stacks* encompasses a large number of structures (also referred to as *multisection quarter-wave transformers*) that are used in a variety of band-limited impedance transformation applications [10], [11]. For applications in optics these structures are realized as quarter-wave layered media with the section impedances varied by using nonmagnetic materials with different refractive indexes. The most common uses here are narrow band antireflective (AR) coatings and high-reflectivity (HR) mirrors. The quarter-wave section refractive indices of an AR coating are typically made to vary monotonically, typical examples being the binomial and Chebyshev transformers [10], [11]. A high-reflection coefficient at the design frequency can be achieved by using a structure in which the refractive index of every

Manuscript received May 24, 1991; revised September 20, 1991. This work was supported by DARPA and Rome Laboratories.

The authors are with the Department of Electrical and Computer Engineering, University of California, Santa Barbara, CA 93106.

IEEE Log Number 9105182.

0018-9197/92$03.00 © 1992 IEEE

Authorized licensed use limited to: Stanford University. Downloaded on January 16, 2009 at 19:40 from IEEE Xplore. Restrictions apply.

subsequent layer alternates in magnitude. In this way all of the reflected waves interfere constructively at the design frequency and produce a high-reflection coefficient with a phase exactly zero or π. Very high peak reflection coefficients ($>99\%$) can be achieved practically in this manner even though it is not theoretically possible to achieve unity reflection coefficient with a finite number of layers [6]. The structure that is most commonly referred to as *the* QWM is a multisection quarter-wave structure in which the section refractive indexes alternate between two fixed values: high n_H and low n_L. Due to its periodic nature the QWM structure is the most common realization of HR coatings in optics and is of primary interest in this paper.

In semiconductor optoelectronics, HR reflectors appear as in-plane and vertical structures. In-plane reflectors constitute distributed feedback and distributed Bragg reflector lasers [5] and are typically fabricated by e-beam lithography and holographic means. The resulting refractive index variation in these structures is typically graded and very weak, and can be efficiently analyzed by perturbation methods such as CWT [6], [7]. The fabrication of vertical HR reflectors involves deposition of quarter-wave layers of alternating refractive indexes by epitaxial growth, evaporation, or plasma deposition. The large variety of materials used for mirror fabrication yields a large range of available refractive index values. Semiconductor mirrors fabricated by crystal growth techniques (MBE, CBE, MOVPE) typically have abrupt refractive index variations across the section boundaries (even though they may be graded [12]) and the materials yield refractive indexes in the range between 3.0 and 3.6. The fractional bandwidth ($\Delta\omega/\omega_0$) of a QWM depends on the refractive indices of the two materials used [13]:

$$\frac{\Delta\omega}{\omega_0} = \frac{4}{\pi}\arcsin\left(\frac{n_H - n_L}{n_H + n_L}\right) \tag{1}$$

and hence the largest $\Delta\omega/\omega_0$ for these epitaxial mirrors is approximately 10%. Evaporation and plasma (PECVD, sputtering) deposition techniques offer a wide range of insulating materials with lower refractive indexes: from $n \sim 1.4$ (MgF_2, SiO_2) to $n \sim 2.35$ (ZnO, TaO_2), and high index materials, such as amorphous semiconductors ($n \sim 3.5$). The fractional bandwidths of amorphous mirrors may exceed 30%. In the case of such large refractive index differences, one needs to solve for the reflectivity spectrum exactly, most commonly by the transmission matrix approach [8], [9].

The phase properties (dispersion and delay) of quarter-wave mirrors have been studied extensively for applications in high-speed lasers [2], [14]–[16]. At the center of the mirror band-stop the dispersion is zero and the reflection delay is at a minimum. Both quantities increase in magnitude for frequencies away from the center. The reflectivity amplitude and phase spectra of a Si_3N_4/Si quarter-wave mirror are shown as an example in Fig. 1. Fig. 2 shows the reflection delay and dispersion dependence on frequency in the neighborhood of the band-stop frequency. The modulation of semiconductor lasers produces optical bandwidths that are very small compared to typical QW mirror bandwidths, and hence we need not consider the dispersion as the limiting parameter in the high-speed operation. In VCSEL, a more severe effect on the operating conditions results from the shift of the laser emission mode due to temperature and fabrication tolerances to a region of longer delay time and lower reflectivity. The rate of change in both of these parameters depends on the amount of mirror dispersion and bandwidth [14]: narrow bandwidth mirrors inherently have very frequency-dependent phase characteristics. The allowed laser emission mode drift will hence place the most stringent requirements on the spectral response of the QW mirror. The devices of our primary interest are vertical cavity surface-emitting lasers that utilize both semiconductor and amorphous dielectric mirrors, hence this report is intended to provide quarter-wave mirror design tools for this application.

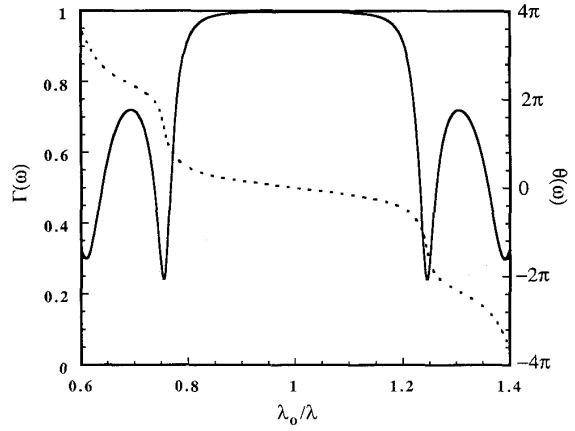

Fig. 1. Calculated amplitude and phase reflectivity spectrum of a five-period quarter-wave mirror centered at $\lambda_0 = 1.3$ μm. The refractive indices are $n_I = 3.2$ (InP), $n_H = 3.5$ (Si), $n_L = 2.0$ (Si_3N_4), and $n_E = 1.0$ (air). No loss or material dispersion is considered for simplicity.

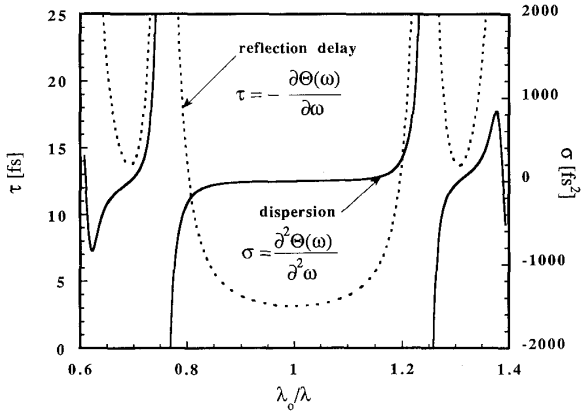

Fig. 2. Calculated reflection delay and dispersion of the quarter-wave mirror shown in Fig. 1.

Authorized licensed use limited to: Stanford University. Downloaded on January 16, 2009 at 19:40 from IEEE Xplore. Restrictions apply.

III. Reflection Delay and Phase Penetration Depth L_τ

The quarter-wave mirror exhibits a complicated phase and amplitude spectrum due to its distributed (multireflection) nature. The most practically useful portion of the mirror spectrum is at or in the immediate neighborhood of the *antiresonance* frequency, i.e., the center of the principal band-stop region. The antiresonance consists of the fact that the round trip phase within each layer in the mirror at that frequency equals an odd multiple of π. The center frequency is also referred to as the Bragg frequency. The spectrum is periodic: the high-reflectivity stop band repeats every odd multiple of the Bragg frequency. For a lossless mirror, the maximum value of the reflectivity occurs at the stop-band center and can be calculated using well-known quarter-wave transformation formulas [6]. We describe here the derivation of the reflection delay at the center frequency for the QWM's with no material loss or dispersion. We assume that the presence of mirror material loss affects the laser operation predominantly through the reduction of the peak reflectivity, rather than the variation of the reflection delay. The reduction of peak reflectivity as a function of material loss will be discussed in Section V. The frequency and time response of dielectric mirrors is described by its complex amplitude reflectivity spectrum:

$$\tilde{\Gamma}(\omega) = \Gamma(\omega) e^{j\Theta(\omega)} \tag{2}$$

where $\Gamma(\omega)$ and $\Theta(\omega)$ are real functions. (The tilde ˜ denotes a phasor). The QWM is a passive linear network and, as such, exhibits a *real* impulse response. It is a straightforward task to show, using the inverse Fourier transform, that for a real impulse response the amplitude spectrum $\Gamma(\omega)$ is an even function, whereas the phase $\Theta(\omega)$ is an odd function of the frequency. For a lossless mirror with no material dispersion this is also true around the center frequency ω_0 where, as a consequence, the phase characteristic has an inflexion [9], seen in Fig. 1. For continuous signals at frequency ω_0 the QWM can be characterized by two parameters: the reflectivity $\Gamma(\omega_0)$ and the phase, which for a QW stack is either zero or π at the center frequency. When the carrier is modulated, both the reflected signal amplitude and the phase are determined by the portion of the mirror reflectivity spectrum that overlaps with the modulated signal spectrum. As Figs. 1 and 2 show, for very narrow modulation bandwidths close to the center of the mirror band stop the relevant portion of the spectrum can be assumed to have uniform amplitude and a linear phase:

$$\tilde{\Gamma} = \Gamma(\omega_0) e^{-j(\omega - \omega_0)\tau} \tag{3}$$

where τ is the *reflection delay* at frequency ω_0 given by

$$\tau = -\left.\frac{\partial \Theta(\omega)}{\partial \omega}\right|_{\omega = \omega_0}. \tag{4}$$

The quantity τ is the time by which an input pulse will be delayed upon reflection [14], also called group-delay time. The fixed-phase term $\Theta(\omega_0)$ present in (2) has been included into the amplitude $\Gamma(\omega_0)$ of (3) for simplicity of upcoming mathematical derivations. The sign of $\Gamma(\omega_0)$ can then take both positive and negative values depending on the orientation of the stack. (The phase of the QW stack at the Bragg frequency can be determined from the phase of the first reflection, since all of the reflections are in phase at the center frequency. Refractive index sequence *HL* at the first interface gives $\Gamma(\omega_0) > 0$, whereas the opposite sequence *LH* yields $\Gamma(\omega_0) < 0$.)

A. Derivation of the Reflection Delay τ

In order to calculate reflection delay τ we will derive a recursion relation between the reflection delay τ_m of an m-section stack and the group delay τ_{m-1} of an $(m-1)$-section stack. Let Z_{m-1} be the input impedance of the $(m-1)$-section structure shown in Fig. 3. We now proceed building the stack by adding a quarter-wave layer to the top. The refractive index of the added layer must be of the proper relative magnitude so that the indexes of the overall structure alternate. (It is irrelevant which of the two material indexes is being used, as long as the phase is properly adjusted). Once the refractive index of the mth layer is specified, by knowing Z_{m-1} one can easily determine Γ_{m-1}: the reflectivity of the $m-1$-layer stack as seen from within the added quarter-wave layer, and Z_m: the input impedance of the m-layer stack. With the next quarter-wave layer added we can determine the reflectivity Γ_m and Z_{m+1}, and so on. The reflectivities Γ_m and Γ_{m-1} are then related by

$$\tilde{\Gamma}_m = -\frac{r_m - \tilde{\Gamma}_{m-1} e^{-j2\omega\Delta\tau}}{1 - r_m \tilde{\Gamma}_{m-1} e^{-j2\omega\Delta\tau}} \tag{5}$$

where r_m is the amplitude reflectivity of the interface between the quarter-wave layers $m+1$ and m, and $\Delta\tau$ is one-quarter period time $4f\Delta\tau = 1$ (f is the band-stop center frequency). Using (3) we express Γ_m and Γ_{m-1}:

$$\tilde{\Gamma}_m = \Gamma_m e^{-j(\omega - \omega_0)\tau_m}. \tag{6}$$

We now simplify (5) using a substitution originally due to Yan [17], [20] and discussed in the Appendix. Knowing that $|r_m| < 1$ and that $\tanh(z)$ is analytic along the real axis we set

$$s_m = \tanh^{-1}(r_m) \qquad \tilde{S}_m = \tanh^{-1}(-\tilde{\Gamma}_m e^{-j2\omega\Delta\tau}). \tag{7}$$

Using the $\tanh(z)$ addition rule (A3) we obtain:

$$\tilde{\Gamma}_m = -\tanh(s_m + \tilde{S}_{m-1}). \tag{8}$$

By differentiating (6) and (8) with respect to ω, and evaluating at ω_0, we obtain

$$\left.\frac{d\tilde{\Gamma}_m}{d\omega}\right|_{\omega=\omega_0} = -j\tau_m\Gamma_m \tag{9}$$

$$\left.\frac{d\tilde{\Gamma}_m}{d\omega}\right|_{\omega=\omega_0} = j(\tau_{m-1} + 2\Delta\tau)\left(\frac{1-\Gamma_m^2}{1-\Gamma_{m-1}^2}\right) + \Gamma_{m-1}. \tag{10}$$

Authorized licensed use limited to: Stanford University. Downloaded on January 16, 2009 at 19:40 from IEEE Xplore. Restrictions apply.

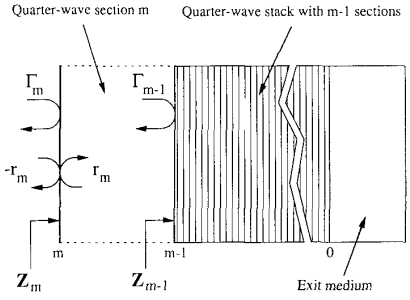

Fig. 3. An $m-1$-section quarter-wave stack with a single quarter-wave layer added on top.

Here we have used the fact that $\Gamma_m(\omega)$ has a maximum at ω_0 and that $\omega_0 \Delta\tau = \pi/2$. Equating (9) and (10) we obtain a recursion relation for the reflection delay τ_m in terms of the delay τ_{m-1} and the associated amplitude reflectivities Γ_m and Γ_{m-1}:

$$\gamma_m \tau_m = \gamma_{m-1}(\tau_{m-1} + 2\Delta\tau) \tag{11}$$

where factors γ_i are given by:

$$\gamma_i = (-1)^i \frac{\Gamma_i}{1 - \Gamma_i^2}. \tag{12}$$

For $m = 0$, the structure reduces to a single interface between the incident and exiting medium: There is no reflection delay and we can set $\tau_0 = 0$. The reflection delay of a single-layer structure τ_1 can now be found from (11). By repeated application of (11) we can similarly find the reflection delay of a QWM of an arbitrary thickness. The recursion relation (11) leads to the sum:

$$\tau_m = \frac{1}{2f} \cdot \frac{\sum_{i=0}^{m-1} \gamma_i}{\gamma_m} \tag{13}$$

Equation (13) is *exact* for *any* multisection quarter-wave transformer at the design frequency, as we have not in any way specified the individual quarter-wave section impedances. In the case of matching transformers, the value of Γ_m is ideally zero, whereas the Γ_i $(i < m)$ are, in general, nonzero. Equation (13) then implies that the reflection delay time is infinite. The physical interpretation would be that the signal never returns, which is indeed the goal of perfect matching. It is possible to generalize this derivation, starting with (5), to arbitrary structures that involve both quarter-wave and half-wave layers. However, in this paper we concentrate only on the QWM structure and refer the reader to reference [20] for a more detailed treatment of the *tanh substitution* and its application in calculating reflectivities of more complex quarter- and half-wave structures.

For the case of a QWM structure (13) can be reduced to an explicit relation due to the simplicity of the relations for the partial reflectivities Γ_i, and hence the factors γ_i. The phase of the reflectivity of every subsequent quarter-wave section alternates between 0 or π, and therefore no generality will be lost by setting

$$\gamma_i = \frac{|\Gamma_i|}{1 - \Gamma_i^2}. \tag{14}$$

We show in the Appendix that γ_i can be written as

$$\gamma_i = \frac{1}{4}\left(\frac{1}{b_i} - b_i\right) \tag{15}$$

where b_i is the product of the low/high refractive index ratios for all interfaces in an i-section stack. For i sections there are $i + 1$ interfaces and b_i is given by

$$b_i = \prod_{k=0}^{i} \left(\frac{n_{Lk}}{n_{Hk}}\right). \tag{16}$$

Expression (13) becomes a sum of two series

$$\tau_m = \frac{1}{2f} \cdot \frac{\sum_{i=0}^{m-1} \left(\frac{1}{b_i} - b_i\right)}{\left(\frac{1}{b_m} - b_m\right)}. \tag{17}$$

Coefficients b_i are all different but can be expressed in a simple way using three parameters: a, p, q, and the number of sections i. Parameters a, p, and q are refractive index ratios of the three types of interfaces that characterize the mirror. All of the ratios are taken as low/high, i.e., a, p, and q are real numbers smaller than 1.

$$q = \frac{n_{LI}}{n_{HI}} \qquad p = \frac{n_L}{n_H} \quad (0 < i < m) \qquad a = \frac{n_{LE}}{n_{HE}}. \tag{18}$$

Factor q is the ratio of the refractive indexes at the interface between the *incident* medium (subscript I) and the *first* QWM section, factor a is the ratio of the refractive indexes at the *last* QWM section and the *exit* medium (subscript E), and factor p is the ratio of the refractive indexes of the two materials that constitute the QWM structure. Using (16) and (18) we find that for $i < m$ we have

$$b_i = \left(\frac{n_{LE}}{n_{HE}}\right)\left(\frac{n_L}{n_H}\right)^i = ap^i \tag{19}$$

and at $i = m$

$$b_m = \left(\frac{n_{LI}}{n_{HI}}\right)\left(\frac{n_{LE}}{n_{HE}}\right)\left(\frac{n_L}{n_H}\right)^{m-1} = qap^{m-1}. \tag{20}$$

Introducing these variables into (17) we are left with a sum of two finite geometric series which, after some manipulation, yield the expression that is the central result of this paper:

$$\tau_m = \frac{1}{2f} \cdot \frac{q}{1-p} \cdot \frac{(1 - a^2p^{m-1})(1 - p^m)}{(1 - q^2a^2p^{2m-2})}. \tag{21}$$

Equation (21) is the exact relation for the reflection delay of a lossless quarter-wave mirror with an arbitrary number of sections and material indexes at the mirror band-stop

Authorized licensed use limited to: Stanford University. Downloaded on January 16, 2009 at 19:40 from IEEE Xplore. Restrictions apply.

center frequency. There are several noteworthy features of (21): The mirror reflection delay is expressed in terms of the magnitude of the individual interface reflections. The value of the delay remains unchanged if q, p, and a are replaced by $1/q$, $1/p$, and $1/a$. This means that any *LHLH* layer sequence has a corresponding *HLHL* sequence for which the delay times are equal. Furthermore, the reflection delay from the front and the back of a QWM is generally not equal as it depends on the incident and exit medium indexes. The functional dependence of (21) is illustrated in Fig. 4 for several number of layers and a continuous variation of the refractive index n_H. The general trend in Fig. 4 is that mirrors with large index differences produce short delay times. The small reduction in the delay for very small index difference occurs because the reflection at the exit medium interface starts dominating (the exit medium in Fig. 4 is air). A fact not apparent in the figure is that any decrease in the refractive index difference for a fixed number of periods will also decrease the maximum reflectivity of the mirror. For a large number of periods the curves approach that of an infinite QWM. The reflection delay of an infinite mirror (unit reflectivity) is the maximum delay a QWM can realize at the center frequency and it is obtained by taking the $m \to \infty$ limit in (21):

$$\tau_\infty = \frac{1}{2f}\left(\frac{n_{LI}}{n_{HI}}\right)\frac{n_H}{n_H - n_L}. \tag{22}$$

It is worth noting that in most amorphous mirrors ($n_H - n_L > 1$) (22) can be used reliably if the number of periods is greater than 3, which can be also seen from Fig. 4. A special case of interest is the behavior of τ_m when the index difference between all of materials involved is a very small n_I, n_E, n_H, $n_L \approx n$, and $\Delta n = n_H - n_L << n$. In this case the reflection delay (and the penetration depth) can be found by differentiating the phase of the expression for the DBR reflectivity obtained by CWT [5]:

$$\tau = \frac{n}{c}\frac{\tanh(\kappa l)}{\kappa} \tag{23}$$

where l is the thickness of the mirror and κ is the coupling coefficient. For a square index perturbation $\kappa = 2\Delta n/\lambda_0$, where λ_0 is the design wavelength ($\lambda_0 = 2\pi c/\omega_0$) [6]. Equation (23) can also be obtained from (21) by applying the noted assumptions about the values of the refractive indices. To this end we let $n_H \approx n + \Delta n/2$ and $n_L \approx n - \Delta n/2$, and set $qa \approx a^2 \approx p$. Equation (21) then reduces to

$$\tau_m = \left(\frac{1}{2f}\right)\frac{q}{1-p}\cdot\frac{(1-p^m)}{(1+p^m)}. \tag{24}$$

Factor p can be approximated by $p^m \approx (1 - \Delta n/n)^m$, whereas the thickness of the mirror is related to m by $l = m\lambda/4n$. We let Δn become very small while keeping κl constant:

$$p^m = \lim_{m\to\infty}\left(1 - \frac{2\kappa l}{m}\right)^m = e^{-2\kappa l}. \tag{25}$$

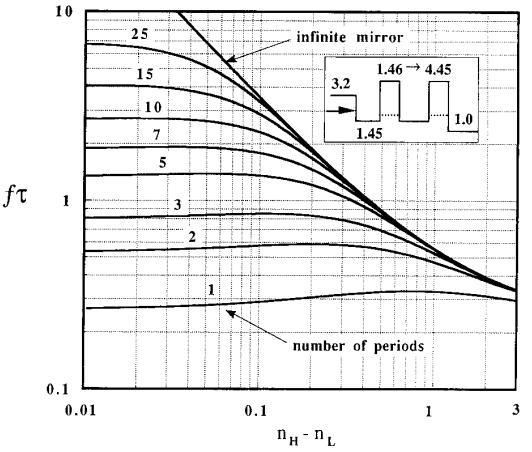

Fig. 4. A family of curves illustrating the functional dependence of normalized reflection delay $f\tau$ on material parameters. The values used in this plot are $n_I = 3.2$ (InP), $n_E = 1.0$ (air), and $n_L = 1.45$ (SiO_2), whereas the refractive index difference $n_H - n_L$ was varied continuously from 0.01 to 3.0 for illustration. The multiple curves correspond to different number of periods: 1, 2, 3, 5, 7, 10, 15, 25, and infinite.

Using (24) and (25) we easily arrive at (23), which shows that in this limit (21) and the results of the CWT agree. The importance of (21), then, lies in its application to abrupt multilayered structures with large index differences such as amorphous dielectric media where the coupled mode theory cannot be applied.

B. The Phase Penetration Depth L_τ

The reflection delay in a distributed reflector is most commonly associated with an *apparent* depth of penetration into the mirror. The interpretation of the delay *time* with *distance* is potentially misleading since one needs to know the *velocity* of propagation in the medium. Nevertheless, for the practical use of the penetration depth concept one never needs the real propagation constant in the medium. The penetration depth is parameter used to model the distributed (approximate linear phase) reflector with a fixed-phase mirror at some distance farther into the original mirror. For simplicity one assumes that the light propagates at the same rate in the reclaimed space in the mirror as in front of the mirror. Fig. 5 illustrates this interpretation: A wave is incident from a medium with refractive index n onto a distributed mirror with linear phase. Its reflection is delayed by τ and scaled by the value of the reflectivity Γ_m. The equivalent model for the distributed mirror is realized by extending the incident medium beyond the reference plane and by placing a fixed-phase mirror at depth L_τ. To the observer placed to the left of the reference plane, the mirrors will appear equivalent if the reflectivity and the phase characteristics of the two cases are equal. It is easy to show that this is satisfied if

$$L_\tau = \frac{c\tau}{2n} \qquad \Theta_0 = \omega_0\tau \tag{26}$$

Authorized licensed use limited to: Stanford University. Downloaded on January 16, 2009 at 19:40 from IEEE Xplore. Restrictions apply.

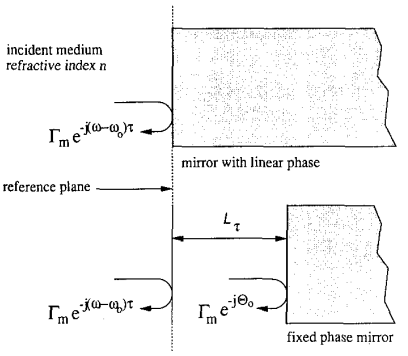

Fig. 5. The illustration of the penetration depth concept. A linear phase mirror is replaced by a fixed phase mirror displaced by length L_τ into the mirror. The linear term in the phase characteristic is absorbed by the distance L_τ, whereas the Θ_0 term assures that the phase of the equivalent and the original mirror match at the center frequency.

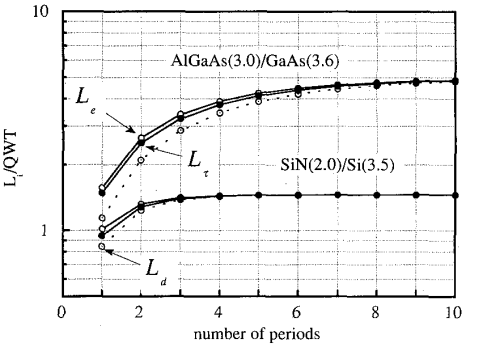

Fig. 6. The comparison between the penetration depths L_e, L_τ, and L_d for two practical quarter-wave mirrors: SiN-Si and AlGaAs-GaAs. The penetration depths are normalized to one quarter-wavelength (QWT) in the incident medium. The refractive indexes of the materials are given in parentheses. The exit medium is air $n_E = 1.0$, and the incident medium InP and GaAs, respectively.

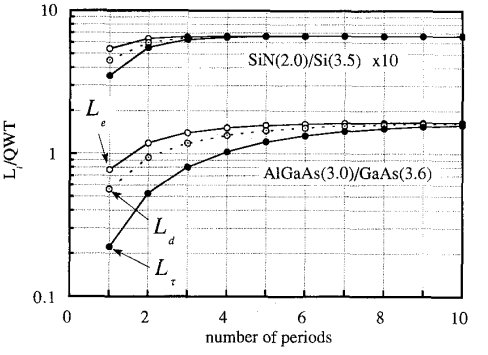

Fig. 7. The comparison between the penetration depths L_e, L_τ, and L_d for the same mirrors as in Fig. 6 except that the incident medium is air $n_I = 1.0$, and the exit medium InP and GaAs, respectively.

where L_τ is the *phase penetration depth*. The use of the equivalent fixed-phase mirror and the penetration depth concept illustrated in Fig. 5 is completely transparent to any calculations involving the mirror phase as long as the QWM can be assumed to have a uniform amplitude and a linear phase in the spectral range of interest. The functional dependence of L_τ on the number of layers is shown in Figs. 6 and 7. The strength of individual interface reflections directly influences how fast the delay saturates with the number of layers in the mirror. For the case of very small material index differences, the phase penetration depth becomes, [from (23) and (26)],

$$L_\tau = \frac{\tanh(\kappa l)}{2\kappa}. \tag{27}$$

The mirror reflection delay needs to be considered in the determination of Fabry–Perot cavity mode frequencies. Consider a cavity with a mirror-to-mirror distance L_{FP} and two identical quarter-wave mirrors each having a reflection delay τ. (The mirror center wavelength is not necessarily tuned to the cavity mirror-to-mirror optical length.) The longitudinal modes of this structure occur at frequencies at which the round trip phase is an integer multiple of 2π. The sum of phase terms in the cavity round-trip gives

$$2\beta_k(L_{\text{FP}} + 2L_\tau) - 2\omega_0\tau = 2\pi k \tag{28}$$

where β_k is the propagation constant of the kth mode, and ω_0 the QWM center frequency. The term in brackets is defined as the *effective* cavity length: $L_{\text{eff}} = L_{FP} + 2L_\tau$. The penetration depth L_τ is defined by (26) with n being the refractive index of the cavity material. Equation (28) shows that, in general, the longitudinal mode frequencies of a Fabry–Perot cavity with quarter-wave mirrors depend on the penetration depth of the mirrors. The only exception is the resonant mode of a cavity in which both the mirror-to-mirror cavity optical length and the QWM center frequency are tuned to the same frequency. Because the QWM phase at the center frequency is always zero or π, the resonant mode frequency and its wave pattern remain intact when the mirror penetration depth is changed. (In (28) L_τ is eliminated for $\beta_k = n\omega_0/c$.) All other modes in this case shift away or toward the design frequency when L_τ is changed.

IV. Energy Penetration Depth L_e

In Section III the concept of penetration depth was introduced in connection with a phase conserving model of the QWM. Now we introduce the *energy penetration depth* L_e, a parameter that relates the total electromagnetic energy stored in the QWM to the energy density in front of the mirror, thus serving as a parameter in an energy-conserving model.

In Fig. 8 we show the energy density distribution in a QWM at the center frequency. The energy distribution within each section is represented by a constant value, whereas the horizontal axis is the number of quarter-wavelengths, which is why all of the mirror sections are shown with equal thicknesses. We first introduce the *normalized energy penetration depth* Λ as the ratio of the to-

Authorized licensed use limited to: Stanford University. Downloaded on January 16, 2009 at 19:40 from IEEE Xplore. Restrictions apply.

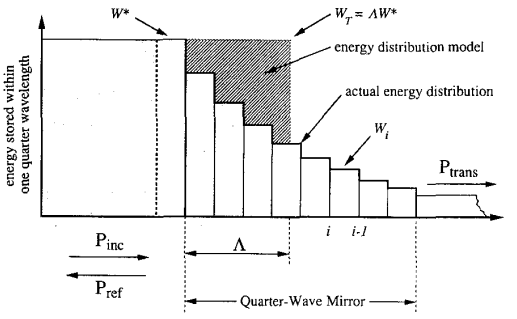

Fig. 8. Energy distribution inside a quarter-wave stack at the band-stop frequency f. The horizontal axis is normalized to the optical path so that all layers have equal width and the energy-per-layer distribution falls monotonically.

tal amount of energy within the mirror W_T and the energy contained in the quarter-wavelength of space in front of the mirror W^*.

$$\Lambda = \frac{W_T}{W^*}. \tag{29}$$

The meaning of Λ is illustrated graphically in Fig. 8: The total energy contained in the blocks of monotonically decreasing height is now contained in a uniform distribution vanishing abruptly at depth Λ. The penetration depth is a dimensionless parameter that expresses width of this distribution in terms of quarter-wave thicknesses. In order to determine Λ we first find the expression for the total energy W_T. Using the notation from Fig. 8, the Poynting vector magnitude in each section S_i vector is given by

$$S_i = |\vec{E}_i \times \vec{H}_i| = \frac{n_i}{Z_0} |E_i|^2 (1 - R_{i-1}) \tag{30}$$

where Z_0 is the characteristic impedance of vacuum, n_i the refractive index of section i and R_{i-1} the power reflectivity of the $i-1$-section quarter-wave mirror seen from the section i. The energy contained in section i is obtained by integrating the energy density over one quarter-wave period:

$$W_i = \frac{n_i}{4 f Z_0} |E_i|^2 (1 + R_{i-1}). \tag{31}$$

In a QWM with no loss, the Poynting vector is constant throughout the structure $S_i = S$. This condition gives us the means of connection between (30) and (31), yielding

$$W_i = \frac{S}{4f} \cdot \frac{1 + R_{i-1}}{1 - R_{i-1}}. \tag{32}$$

The total energy in the mirror is now a sum of all W_i. We just need to sum (32) for all sections in the mirror. Using the *tanh substitution*, again with (A11) and (20), we have

$$W_i = \frac{S}{8f} \left(\frac{1}{b_{i-1}} + b_{i-1} \right). \tag{33}$$

The penetration depth Λ is then given by the sum,

$$\Lambda = \frac{\sum_{i=0}^{m-1} \left(\frac{1}{b_i} + b_i \right)}{\left(\frac{1}{b_m} + b_m \right)}. \tag{34}$$

By the introduction of a, q, and p after some manipulation we arrive at

$$\Lambda = \frac{q}{1 - p} \cdot \frac{(1 + a^2 p^{m-1})(1 - p^m)}{(1 + q^2 a^2 p^{2m-2})}. \tag{35}$$

This expression is exact for an arbitrary QWM at the center frequency. Note the similarity with (21): The difference arises from the distributed nature of the quarter-wave mirror. We can now define the *energy penetration depth* with the dimensions of distance as

$$L_e = \frac{\lambda_0}{4n} \Lambda. \tag{36}$$

The general behavior of Λ as a function of mirror refractive indexes is very similar to the one shown for $f\tau$ in Fig. 4. By taking the ratio of (21) and (35) one can see that for a finite m, L_e is always greater than L_τ. The two penetration depths become practically equal if $a^2 p^m \ll 1$ and the difference between them decreases with the degree by which this condition is met. Physically this means that either the number of layers is large, in which case $p^m \to 0$, or the last interface in the mirror dominates the overall reflectivity: ($a \ll 1$). The effect can be seen by comparing Figs. 6 and 7 where we have shown L_e and L_τ as function of the number of periods ($2m$) for an epitaxial and an amorphous mirror sandwiched between a semiconductor and air. In Fig. 6 the incident medium is the semiconductor, whereas in Fig. 7 it is air. The factor a^2 in Fig. 6 is almost five times smaller than in Fig. 7 and therefore the two penetration depths in Fig. 6 are almost equal for all numbers of periods. In the small-index difference limit using the approximations described in (24) and (25) we can show that

$$L_e = \frac{\tanh(2\kappa l)}{2\kappa} \tag{37}$$

which also shows that $L_e > L_\tau$ for short mirrors. The discrepancy between the two penetration depths (27) and (37) is most significant in the limit $\kappa l \to 0$. For small κl the energy distribution in the mirror is close to uniform and therefore $L_e \to l$. Because the reflection delay is an average of reflections from all interfaces, it is natural to expect that $L_\tau \to l/2$ in the $\kappa l \to 0$ limit. An example of the use the energy penetration depth is the determination of the longitudinal confinement factor in a VCSEL. The confinement factor is given by the ratio of electromagnetic energy in the active region of length L_a and the total energy present in the cavity:

$$\Gamma_L = \frac{L_a}{L_{FP} + 2L_e} \tag{38}$$

Authorized licensed use limited to: Stanford University. Downloaded on January 16, 2009 at 19:40 from IEEE Xplore. Restrictions apply.

and therefore the penetration depth to be used when calculating the cavity mode separation and the longitudinal confinement factor is not the same for finite mirrors.

V. Absorptance

VCSEL laser mirrors typically require reflectivity values in excess of 98% for efficient operation. Because the cavity mirror losses are proportional to $\ln(R) \sim 1 - R$, any small variation of R produces large changes in the loss [21]. The determination of the peak reflectivity of a mirror with no loss is a simple task using the quarter-wave transformation equations [6], [20], but the predicted values provide an overestimate of the value of the reflectivity if loss is present in the mirror. The reasons for the reduction of the peak reflectivity arises from the scattering at rough interfaces between the sections or most commonly from the absorption in the dielectric materials that constitute the mirror. Given that the extinction coefficients are known for all mirror materials, the exact value of the reflectivity can be obtained using the transmission matrix approach [8], [9]. There are, however, approximate expressions that are valid in the case of small loss and very long mirrors [13]. Our objective is to derive an analytic expression for the absorptance of the QWM with weak absorption loss as a function of mirror optical parameters and the number of layers and relate this to the concept of energy penetration depth and the maximum mirror reflectivity. The derived expressions will also take into account that the absorption loss in the two materials may in general be different.

Consider a QWM with no absorption: Power conservation requires that the sum of the power reflectivity and transmission coefficients equal unity, namely $R_0 + T_0 = 1$. If there is power dissipation present in the mirror, then both the reflectivity and the transmission will be reduced. The power balance is now given by $R + T + A = 1$, where R and T are the reflectivities of the mirror with loss, and A is the absorptance [13]:

$$A = \frac{P_{\text{diss}}}{P_{\text{inc}}}. \tag{39}$$

Here P_{diss} and P_{inc} are the power dissipated and power incident on the reflector. For small loss we assume that the reflectivity and the transmission can be approximated by

$$R \approx R_0(1 - A) \qquad T \approx T_0(1 - A). \tag{40}$$

These relations satisfy the power balance condition $R + T + A = 1$, and because it has been shown [18] that $(R - R_0)/R_0$ and $(T - T_0)/T_0$ are of the same order, they represent a reasonable first-order approximation for the reduced reflectivity value. For high-reflectivity mirrors the error in estimating R by the use of (40) reduces, as $R >> T$. We now proceed to determine the absorptance of a QWM. Under steady-state conditions the power dissipated in the mirror can be deduced from the energy distribution in the mirror and the loss rate:

$$\frac{dW_T}{dt} = -c \int \frac{\alpha(x)}{n(x)} w(x)\, dx \tag{41}$$

$$W_T = \int w(x)\, dx \tag{42}$$

where the integrals are to be taken over the entire length of the mirror. Here $\alpha(x)$ and $n(x)$ are the position-dependent power loss coefficient (1/length) and the refractive index within the mirror. The energy density per unit length is denoted by $w(x)$ and the total energy present in the mirror by W_T. The QWM structure is periodic with two different materials of equal optical thickness, therefore $\alpha(x)$ and $n(x)$ are uniform within each section. Equations (41) and (42) can then be written as

$$P_{\text{diss}} = -\frac{dW_T}{dt} = 4\pi f \left(\frac{k_L}{n_L} W_L + \frac{k_H}{n_H} W_H \right) \tag{43}$$

where W_L and W_H are the amounts of energy present in the two materials. The material extinction coefficients are denoted by k_L and k_H. (The extinction coefficients are related to the absorption coefficients via $\alpha = 4\pi k/\lambda$). If the extinction coefficients are linear and sufficiently small so that the energy distribution may be assumed unperturbed by the presence of loss, we can estimate the dissipated power by using the unperturbed field distributions in (41) and (43). The problem them amounts to finding the energies W_L and W_H as functions of the incident power P_{inc} and the physical parameters of the QWM. In Section IV we have already determined by relationship between the total energy W_T and the energy in the quarter-wavelength in the front of the mirror W^*. The next step is relating W^* to the incident power P_{inc}. The energy stored in one quarter-wavelength of incident medium in front of the mirror can be found from (32) by setting $i = m + 1$.

$$W^* = \frac{S}{4f} \cdot \frac{1 + R_0}{1 - R_0} \tag{44}$$

where $R_0 = R_m$ is the reflectivity of the complete QWM:

$$R_0 = \left(\frac{1 - aqp^{m-1}}{1 + aqp^{m-1}} \right)^2. \tag{45}$$

The Poynting vector can be related to the incident power via

$$S = P_{\text{inc}}(1 - R_0) \tag{46}$$

and finally, using (39) and (43), we arrive at

$$A = \pi(1 + R_0) \left[\left(\frac{k_L}{n_L} \right) \frac{W_L}{W^*} + \left(\frac{k_H}{n_H} \right) \frac{W_H}{W^*} \right]. \tag{47}$$

The evaluation of W_L and W_H in terms of W^* can, in principle, be done by separating the odd and the even terms in the summation (34), taking care that the final expressions will differ depending on the parity of m. There is, however, a simpler way to obtain the fractions of power

Authorized licensed use limited to: Stanford University. Downloaded on January 16, 2009 at 19:40 from IEEE Xplore. Restrictions apply.

in materials H and L by using the expression for normalized penetration depth Λ. Consider (32) for energy stored in section i and the expressions for the peak reflectivity of a QWM (A8) and (A9). Suppose that one of the refractive indexes, for example n_L, changed sign to $-n_L$. Under this transformation Γ_i remains unchanged if $n_{i-1} = n_H$, but $\Gamma_i \to 1/\Gamma_i$ if $n_{i-1} = -n_L$. This alteration then changes the sign of the quantity W_i in (32) only for layers for which $n_{i-1} = -n_L$. Consequently, we can determine the difference between the total energy present in materials H and L by replacing n_L by $-n_L$ in (35). Using this simple trick, both W_L and W_H can be found by the application of (35) with different signs in front of for n_L and n_H. For this purpose let us indicate the explicit dependence of Λ on the material refractive indexes n_L and n_H by writing $\Lambda = \Lambda_m(n_H, n_L)$. The W_L and W_H are then given by

$$W_L = \tfrac{1}{2}[\Lambda_m(n_L, n_H) + \Lambda_m(n_L, -n_H)]\,W^* \tag{48}$$

$$W_H = \tfrac{1}{2}[\Lambda_m(n_L, n_H) + \Lambda_m(-n_L, n_H)]\,W^*. \tag{49}$$

The functional dependence of W_L/W_T and W_H/W_T is illustrated in Fig. 9. As expected, the top layer material always contains more energy than the bottom, hence fabricating mirrors in such a way that the top layer is the one with lower absorption will produce higher reflectivity. Recognizing that $\Lambda_m(n_H, -n_L) = -\Lambda_m(-n_H, n_L)$, we finally have the expression for absorptance:

$$A = \frac{\pi}{2}(1 + R_0)\left[\left(\frac{k_L}{n_L} + \frac{k_H}{n_H}\right)\Lambda_m(n_L, n_H) + \left(\frac{k_L}{n_L} - \frac{k_H}{n_H}\right)\Lambda_m(n_L, -n_H)\right]. \tag{50}$$

The first term in (50) is the contribution from the average loss in the mirror, whereas the second represents the correction for the difference in the loss rates between the two types of layers. In the limit of small loss ($n_i \gg k_i$) this expression gives the correct value of the QWM absorptance for any combination of refractive indexes and number layers. It is instructive to investigate the behavior of (50) for very long mirrors, i.e., $m \to \infty$. The penetration depth saturates at $\Lambda = q/(1 - p)$, but to obtain the absorptance we need to note the orientation of the quarter-wave sequence. For the case when the first layer in the mirror is of material H the absorptance becomes

$$A = 2\pi\,\frac{(k_H + k_L)}{(n_H + n_L)} \cdot \frac{n_I}{(n_H - n_L)}. \tag{51}$$

Similarly, for an infinite mirror with material L as the first layer we obtain

$$A = \frac{2\pi}{n_I(n_H - n_L)} \cdot \frac{(n_L^2 k_H + n_H^2 k_L)}{(n_H + n_L)}. \tag{52}$$

These two expressions are known approximate relations for the absorptance of the quarter-wave stack in the presence of small loss given in [13], [18], [19]. Equation (50)

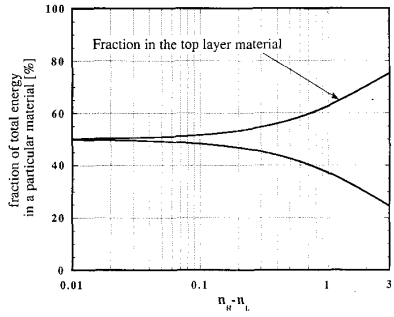

Fig. 9. Calculated distribution of total energy in the mirror between the two mirror materials: The top material always contains more energy. The structure is identical to the one used in Fig. 1.

is a general result applicable to quarter-wave mirrors of any number of layers (odd or even) and optical parameters of both the mirror materials and the surrounding media. The absorptance of a quarter-wave stack with weak absorption was also estimated by D. J. Hemingway and Lissberger [19] using a different method. Their approach yielded two absorptance expressions that differed depending on whether the total number of layers is odd or even and assumed that the incident and the exit medium refractive indexes equal to one of the mirror material indexes. Both of the absorptance expressions given in [19] can be obtained from (50) by evaluating Λ_m for a particular parity of m. Using the approximation (40), (50) can be used to find the reduction in QWM peak reflectivity due to the presence of weak absorptance. Fig. 10 shows the calculated peak reflectivity for the quarter-wave mirror structure shown in the inset of Fig. 4 with and without absorption loss in the silicon layers. The reflectivity calculation has been done exactly using transmission matrix approach [9] and using the approximate expression for reflectivity (40) with the absorptance given by (50). For the case shown there was practically no difference between the two methods of calculation, in spite of the relatively high extinction coefficient used for amorphous silicon ($k_H = 0.01$ @ 1.3 μm). At this point one may wish to interpret the absorptance as a product of the an average material absorption coefficient (independent of the number of layers) and a penetration depth. However, it is not possible to realize this kind of a separation unless the second term in (50) is neglected. In that case the absorptance can be written as

$$A \approx 2\bar{\alpha}L_d \tag{53}$$

where

$$\bar{\alpha} = \frac{n_L\alpha_H + n_H\alpha_L}{n_L + n_H} \tag{54}$$

and L_d is the *loss (dissipative) penetration depth* given by

$$L_d = \left(\frac{\lambda_0}{4n}\right)\frac{q}{1 - p} \cdot \frac{(1 + a^2p^{m-1})(1 - p^m)}{(1 + qap^{m-1})^2}. \tag{55}$$

Note the difference between the denominators of L_d and L_e. It arises from the presence of the $(1 + R_0)$ term in

Authorized licensed use limited to: Stanford University. Downloaded on January 16, 2009 at 19:40 from IEEE Xplore. Restrictions apply.

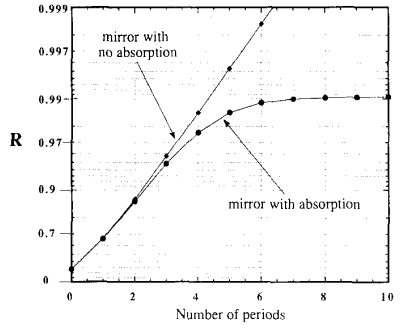

Fig. 10. The comparison between the peak reflectivities of Si_3N_4-Si mirrors both with no loss present in silicon and with absorptive silicon using (50). The refractive indexes used were $n_L = 2.0$ (Si_3N_4) and $n_H = 3.5 - i0.01$ (Si, $\lambda_0 = 1.3$ μm).

(50). Figs. 6 and 7 compare the loss penetration depth L_d to L_e and L_τ for two practical mirrors, and as expected from expressions (35) and (55) $L_e > L_d$ always. For mirrors with a small index difference we can solve for L_d both using CWT and from (55) by introducing approximations (24) and (25):

$$L_d = \frac{\tanh(\kappa L)}{2\kappa}. \tag{56}$$

Equation (56) is identical to (27) and therefore for mirrors with small index differences (practical epitaxial mirrors) one can use either L_τ or L_d when calculating the absorptance. An example of the use of our absorptance derivations is the accounting for mirror loss in the laser threshold gain determination. Consider a Fabry–Perot cavity with a mirror to mirror cavity length L_{FP} and two identical mirrors with peak power reflectivity of R. The active region and the cladding thickness are L_a and L_c, respectively, and the lateral confinement factor is Γ. The threshold gain is then given by

$$\Gamma g_{th} L_a = \Gamma \alpha_a L_a + \Gamma \alpha_c L_c - \ln(R_d) - \ln(R) \tag{57}$$

where α_a, α_c, $-\ln(R_d)$, and $-\ln(R)$ are the losses in the active and the cladding regions, the diffraction losses, and the mirror losses. Reflectivity R in this expression includes the mirror loss and therefore there is no need for introducing a penentration depth. In practice, the reduction of reflectivity due to the presence of loss is very small and the logarithm can be expanded in order to separate the interference and the dissipative part of the $-\ln(R)$ term. Using (40) we have

$$-\ln(R) = -\ln(R_0) + 2\bar{\alpha} L_d \tag{58}$$

where R_0 is the reflectivity of the laser mirror is lossless. Introducing (58) back to (57) we obtain the threshold gain expression most commonly used for epitaxial mirrors.

VI. Conclusion

In this paper we have discussed the significance of the quarter-wave mirror *penetration depth*, as a parameter both in a phase and an energy conserving model of the quarter-wave mirror. The *reflection delay* is the origin of the phase penetration depth L_τ and it plays a role in the determination of the cavity mode position and separation, whereas *energy penetration depth* L_e is used to evaluate the longitudinal confinement factor in a vertical cavity surface-emitting laser structure. In our study we concentrated only on the mirror properties at and in the immediate neighborhood of the Bragg frequency. For this condition we have derived exact analytic expressions for both L_e and L_τ valid for arbitrary index differences and number of layers, which makes our expressions applicable to both epitaxial and amorphous quarter-wave mirrors. We furthermore show that the difference between L_e and L_τ reduces with the number of sections in the mirror and the strength of the reflection at the last mirror interface. In the limit of an infinitely long mirror L_e and L_τ become equal. The derived expressions agree with the predictions of the CWT in the limit of small refractive index differences. We have also used the energy penetration concept to derive a first-order approximation for the absorptance of a quarter-wave stack in the limit of small loss and related the concepts to the threshold gain calculation for a VCSEL. The *loss penetration depth* L_d was introduced as parameter that approximately accounts for the effect of small absorption loss in the mirror on the value of the peak reflectivity.

Appendix

The *tanh* substitution provides a simple way to determine the reflectivity of combinations of quarter-wave and half-wave multilayer structures at the resonant frequency. We illustrate here the use of the substitution applied to the quarter-wave mirror case. For more general applications the reader is referred to [20] where the tanh substitution has been discussed in detail.

We start from the same consideration as in (5), except that for the peak reflectivity calculation we do not have to use complex reflectivities. Consider the reflection of a single quarter-wave layer structure. Equation (5) then reads

$$\Gamma_1 = \frac{r_1 + \Gamma_0}{1 + r_1 \Gamma_0}. \tag{A1}$$

Using the substitution

$$s_i = |\tanh^{-1}(r_i)| \tag{A2}$$

and the hyperbolic tangent addition formula (A10), we arrive at

$$|\Gamma_1| = \tanh(s_1 + s_0). \tag{A3}$$

The relation for the peak reflectivity of the entire stack can be derived by repeated application of (A1), (A3), and (A3):

$$|\Gamma_2| = \tanh(s_2 + s_1 + s_0) \tag{A4}$$

$$\vdots$$

$$|\Gamma_m| = \tanh\left(\sum_{i=0}^{m} s_i\right) \tag{A5}$$

Authorized licensed use limited to: Stanford University. Downloaded on January 16, 2009 at 19:40 from IEEE Xplore. Restrictions apply.

where the summation goes over all interfaces in the structure: for m layers there are $m + 1$ interfaces. Each interface is characterized by a factor s_i, which can be expressed in terms of material indexes at the interfaces: Using (A2), we can write

$$|r_m| = \frac{1 - e^{-2s_i}}{1 + e^{-2s_i}} = \frac{1 - (n_{Li}/n_{Hi})}{1 + (n_{Li}/n_{Hi})} \tag{A6}$$

and find that s_i is given by,

$$s_i = -\frac{1}{2} \ln \left(\frac{n_{Li}}{n_{Hi}} \right). \tag{A7}$$

The reflectivity of the entire structure is then given by

$$\Gamma_m = \frac{1 - b_m}{1 + b_m} \tag{A8}$$

with b_m being the product of the refractive indexes (n_L/n_H) for all interfaces in the stack:

$$b_m = \prod_{i=0}^{m} \left(\frac{n_{Li}}{n_{Hi}} \right). \tag{A9}$$

(Note that $0 < b_m < 1$.) Using identity (A12) it is easy to show that (14) reduces to (15):

A. Hyperbolic Function Identities Used in the Derivations

$$\tanh (a + b) = \frac{\tanh (a) + \tanh (b)}{1 + \tanh (a) \tanh (b)} \tag{A10}$$

$$\cosh (2a) = \frac{1 + \tanh^2 (a)}{1 - \tanh^2 (a)} \tag{A11}$$

$$\sinh (2a) = \frac{2 \tanh (a)}{1 - \tanh^2 (a)}. \tag{A12}$$

ACKNOWLEDGMENT

The authors wish to thank Dr. M. Whitehead, Dr. N. Dagli, Dr. J. E. Bowers, and R. L. Nagarajan for useful discussions.

REFERENCES

[1] A. F. Turner and P. W. Baumeister, "Multilayer mirrors with high reflectance over an extended spectral region," *Appl. Opt.*, vol. 5, no. 1, pp. 69–76, 1966.
[2] P. Laporta and V. Magni, "Dispersive effects in the reflection of femtosecond optical pulses from broadband dielectric mirrors," *Appl. Opt.*, vol. 24, pp. 2014–2020, 1985.
[3] H. Soda, K. Iga, C. Kitahara, and Y. Suematsu, "GaInAsP/InP surface emitting injection lasers," *Japan. J. Appl. Phys.*, vol. 18, pp. 2329–2330, 1979.
[4] R. H. Yan, R. J. Simes, and L. A. Coldren, "Analysis and design of surface-normal Fabry-Perot electrooptic modulators," *IEEE J. Quantum Electron.*, vol. 25, pp. 2272–2280, 1989.
[5] F. Koyama, Y. Suematsu, S. Arai, and T. Tawee, "1.5–1.6 μm GaInAsP/InP dynamic-single-mode (DSM) lasers with distributed Bragg reflector," *IEEE J. Quantum Electron.*, vol. QE-19, pp. 1042–1051, 1983.
[6] H. Haus, *Waves and Fields in Optoelectronics*. Englewood Cliffs, NJ: Prentice-Hall, 1984.
[7] H. Kogelnik and C. V. Shank, "Coupled-wave theory of distributed feedback lasers," *J. Appl. Phys.*, vol. 43, pp. 2327–2335, 1972.
[8] E. Hecht, A. Zajac, *Optics*. Reading, MA: Addison-Wesley, 1974.
[9] A. Thielen, *Design of Optical Interference Coatings*. New York: McGraw-Hill, 1989.
[10] R. E. Collin, *Foundations of Microwave Engineering*. New York: McGraw-Hill, 1966.
[11] —, "Theory and design of wide-band multisection quarter-wave transformers," in *Proc. IRE*, pp. 179–185, 1955.
[12] K. Tai, L. Yang, Y. H. Wang, J. D. Wynn, and A. Y. Cho, "Drastic reduction of series resistance in doped semiconductor distributed Bragg reflectors for surface emitting lasers," *Appl. Phys. Lett.*, vol. 56, pp. 2496–2948, 1990.
[13] H. A. Macleod, *Thin-film optical filters*. Bristol, England: Adam Hilger Ltd., 1986.
[14] S. De Silvestri, P. Laporta, and O. Svelto, "Analysis of quarter-wave dielectric-mirror dispersion in femto-second dye-laser cavities," *Opt. Lett.*, vol. 9, pp. 335–337, 1984.
[15] —, "The role of cavity dispersion in CW mode-locked lasers," *IEEE J. Quantum Electron.*, vol. QE-20, pp. 533–539, 1984.
[16] C. F. Bruce and P. E. Ciddor, "Phase dispersion in multilayer films," *J. Opt. Soc. Amer.*, vol. 50, pp. 295–299, 1960.
[17] R. H. Yan, "High-performance transverse electro-optic modulators using Fabry-Perot modulators," Ph.D. dissertation, University of California, Santa Barbara, 1990.
[18] P. Giacomo, "Les couches reflechissantes multidielectriques appliquees a l'interferometre de Fabry-Perot. Etude theorique et experimentale des couches reelles," *Rev. Opt.*, vol. 35, pp. 317–54, 1956.
[19] D. J. Hemingway and P. H. Lissberger, "Properties of weakly absorbing multilayer systems in terms of the concept of potential transmittance," *Optica Acta*, vol. 20, pp. 85–96, 1973.
[20] S. W. Corzine, R. H. Yan, and L. A. Coldren, "A tanh substitution technique for the analysis of abrupt and graded interface multilayer dielectric stacks," *IEEE J. Quantum Electron.*, vol. 27, pp. 2086–2090, Sept. 1991.
[21] M. Oshikiri, H. Kawasaki, F. Koyama, and K. Iga, "Reflectivity dependence of threshold current in GaInAsP/InP surface emitting laser," *IEEE Photon. Technol. Lett.*, vol. 1, pp. 11–13, Jan. 1989.

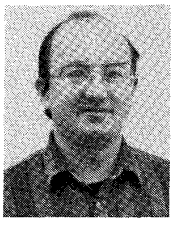

Dubravko I. Babic was born in Zagreb, Croatia, in 1959. He received the Dipl. Ing degree in electrical engineering from University of Zagreb, Croatia, in 1982 and the M.S. degree from the University of California, Santa Barbara, in 1984.

From 1985 to 1989 he was with the Advanced Bipolar Devices Research and Development Department, Avantek Inc, Santa Clara, CA, on the design, modeling, and fabrication of high-speed silicon and GaAs microwave diodes. He is presently working towards the Ph.D. degree at the University of California, on the development of long wavelength vertical cavity surface emitting lasers.

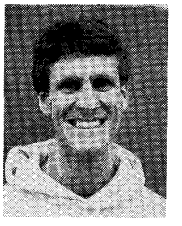

Scott W. Corzine was born in Nashville, TN, in 1963. He received the B.S. and M.S. degrees, both in electrical engineering, from the University of California, Santa Barbara, in 1985 and 1987, respectively.

He is presently working towards the Ph.D. degree at the University of California, with interest focused on the fabrication and design of optoelectronic devices including surface-emitting structures. During the summer of 1987, he was temporarily employed at AT&T Bell Laboratories working on high speed, ultrashort pulse active mode locking in semiconductor lasers.

Authorized licensed use limited to: Stanford University. Downloaded on January 16, 2009 at 19:40 from IEEE Xplore. Restrictions apply.